Lithuanian Journal of Physics
Vol. **64**, No. 1, pp. 1–10 (2024)

ISSN 1648-8504 eISSN 2424-3647
DOI: https://doi.org/10.3952/physics.2024.64.1.1

THE XYZ MODEL IN THE MEAN-FIELD APPROXIMATION IN TERMS OF PAULI SPIN MATRICES

E. Albayrak

Department of Physics, Erciyes University, 38039 Kayseri, Turkey
Email: albayrak@erciyes.edu.tr

Received 18 May 2023; revised 8 June 2023; accepted 9 June 2023

The mean-field approximation (MFA) of spin-1/2 XYZ model was studied by using the Pauli spin matrices and their exponentials which led to very nice hyperbolic tangent functions in nonlinear form. The magnetization components M_x, M_y and M_z were obtained for the ferromagnetic (FM) case and then it was modified for the antiferromagnetic (AFM) case by introducing the sublattices. The bilinear exchange interaction parameters J_x, J_y and J_z, and the external magnetic fields H_x, H_y and H_z were considered along the three-dimensions for various coordination numbers $q = 3, 4$ and 6. The thermal variations of the magnetizations and thus the phase diagrams were obtained to illustrate the behaviours of phase transition lines in the AFM case.

Keywords: spin-1/2, XYZ model, Pauli spin matrices, magnetization, antiferromagnetic, phase diagrams

PACS: 75.10.Hk, 75.30.Kz, 75.50.Gg

1. Introduction

In the study of spin models, the spins are usually assumed to have only discrete values and thus only the possible spin values are used in calculating the magnetization of a given system. The Ising model is such a model in which a spin can be up or down with the possible spin values of ±1/2 along a given direction. But the spins may be aligned in any direction in space making them to be three-dimensional objects. Spins are actually quantum mechanical with the eigenvalues corresponding to the discrete values mentioned above. Since the spins must have the same spin values in all directions, i.e. $S_i^\mu = \pm 1/2$ with $\mu = x, y$ or z, this does not lead to any distinction between the spin directions. The spins are indeed quantum mechanical operators with the eigenvalues corresponding to these discrete values. Thus, one may use the Pauli spin matrices as operators to distinctly separate the possible spin dimensions. This makes the problem more difficult to deal with.

Since the lowest spin system consists of spin-1/2 particles with two states along each axis, it is also the most studied system in the Heisenberg models. It should be noted that when the bilinear interaction parameters along three dimensions are not equal, then the model is called the XYZ model, while when all of them are equal, it is the XXX model, and when two of them are equal but one of them is not, it is named the XXZ model. These models have been studied for many cases by following different theoretical approaches.

The XXX model has been considered mostly for the chain models. The ground state of the isotropic quantum spin chain with a non-diagonal boundary term was proposed by using the Bethe ansatz solution [1]. In addition, a few examples are the rigorous mathematical framework nonperturbative renormalization group (RG) transformations in the finite-temperature regime [2] and the geometric quantum discord for three spin-1/2 particles in the external magnetic field [3]. The critical frontier of the isotropic AFM Heisenberg model in a magnetic field along the z axis was considered by mean field (MF) and effective field theory (EFT) RG calculations [4]. By using the differential operator technique and the EFT scheme, the critical behaviour of amorphous classical Heisenberg ferromagnet in a random field was considered [5].

The XXZ model has been taken into account in many cases, such as the model on a square lattice, studied by using Monte Carlo (MC) simulation to observe the temperature dependences of energy, specific heat and order-parameter [6]. The thermodynamic properties of the model with XY-like anisotropy were examined on the 4×4 square lattice by diagonalization of the Hamiltonian numerically [7]. The cluster-variation method (CVM) was used to examine the phase diagram and the global phase diagrams were calculated for arbitrary values of anisotropy and external magnetic fields [8]. The magnetization process of the AFM models with Ising-like anisotropy in the ground state was investigated [9]. The anisotropic Heisenberg model under AFM interaction was studied by the MF RG approach on a simple cubic lattice [10]. It was studied in a transverse magnetic field and shown that the field induces a gap in the spectrum with the easy-plane anisotropy [11]. The phase diagram of the two-dimensional quantum anisotropic Heisenberg model was considered by adapting an RG approach [12]. The magnetic properties of the Ising-like model on the Shastry-Sutherland lattices with long-range interactions were studied by using the quantum Monte Carlo (MC) method [13]. The ground state magnetic phase diagram of the one-dimensional anisotropic model in the presence of transverse uniform and staggered magnetic fields was considered [14]. The ground-state properties of the quasi-one-dimensional AFM Heisenberg model were investigated by using a variational method [15]. The quantum phase transition, scaling behaviours, and thermodynamics on a honeycomb lattice were systematically studied using the continuous-time quantum MC method [16]. Magnetization plateau and supersolid phases were analyzed in the AFM Heisenberg model on a tetragonally distorted fcc lattice [17]. The anisotropic Heisenberg AFM model in the presence of a Dzyaloshinskii–Moriya (DM) interaction and a uniform longitudinal magnetic field was given [18]. The anisotropic AFM Heisenberg model in the presence of a longitudinal external magnetic field and a DM interaction was studied by employing the usual approximation (MFA) [19].

Lastly, the XYZ models were also examined in many cases. The FM case in a transverse field and uniform long-range interactions among z-components of spins was studied using the MF Jordan–Wigner transformation [20]. The quantum phases of an anisotropic Heisenberg chain under a uniform and staggered magnetic field were examined [21]. The Ising–Heisenberg model with the pair of Heisenberg and quartic Ising interactions was exactly solved by establishing a precise mapping with the corresponding zero-field eight-vertex model [22]. The model with both periodic and anti-periodic boundary conditions was studied via the off-diagonal Bethe ansatz method [23]. The classical Heisenberg model on a simple cubic lattice was investigated by the EFT based on a two-spin cluster [24]. The quantum phase transition of the Heisenberg model with DM interaction via the infinite matrix product state representation with the infinite time-evolving block decimation method was investigated [25]. Magnetic and thermodynamic properties of the anisotropic XYZ finite chain under both homogeneous and inhomogeneous magnetic fields were theoretically studied at low temperature [26]. A quantum refrigerator based on an anisotropic two Heisenberg XYZ model in external magnetic fields with the DM interaction was suggested [27]. A high-temperature series expansion code for the Heisenberg model was presented on arbitrary lattices [28]. Thermal entanglement was considered in the anisotropic Heisenberg model with DM interaction in an inhomogeneous magnetic field [29]. The Heisenberg model was formulated in terms of the usual MFA by using the matrix forms of spin operators in three dimensions [30].

It should be noted that many body problems can be approached by converting them to an easily solvable one-body problem by considering a chosen spin at a given site i placed into an effective medium that creates a local magnetic field H_i at the site i. Therefore, the chosen spin interacts with an MF induced by all other spins and with possible external parameters. Although this approximation does not yield exact results, at least it does give us some qualitative results which may be guiding us in developing better theories in the approach to the problem.

In this work, instead of using the approach of the MFA given in Ref. [30], we use the exponentials of Pauli spin matrices and their series expansions [31], and then they are simplified by the application of the commutation and anti-commutation relations to obtain a very nice form of the magnetization components in three dimensions. The thermal variations of magnetizations are studied for the AFM case by dividing the lattice into sublattices to obtain the phase diagrams for the given coordination numbers $q = 3$, 4 and 6.

The rest of the work is set up as follows: Section 2 contains the formulation in detail, and Section 3 demonstrates the thermal variations of magnetization components and phase diagrams. Those are followed by the conclusions and the Appendix presenting the details of calculations.

2. Pauli spin matrices for the MFA in the XYZ model

We take into account the XYZ model which is assumed to have the following Hamiltonian:

$$\mathcal{H} = -\sum_{\langle i,j\rangle} J_x S_i^x S_j^x - \sum_{\langle i,j\rangle} J_y S_i^y S_j^y - \sum_{\langle i,j\rangle} J_z S_i^z S_j^z - \sum_i H_x S_i^x - \sum_i H_y S_i^y - \sum_i H_z S_i^z, \tag{1}$$

where S_i^x, S_i^y and S_i^z are the spin-1/2 matrices, J_x, J_y and J_z are the bilinear exchange interaction parameters between the nearest-neighbour (NN) spins, and H_x, H_y and H_z are the external magnetic fields along the x, y and z directions, respectively. The model is called the XYZ model when $J_x = J_y = J_z$, it turns into the XXX model when $J_x \neq J_y \neq J_z$ and it becomes the XXZ model when $J_x = J_y \neq J_z$.

We rewrite the Hamiltonian in the MFA by considering a single selected spin i and its interactions with its neighbouring spins and with the external parameters in the following form

$$-\beta\mathcal{H}_{\mathrm{MFA}}^{(i)} = \beta[(qJ_xM_x + H_x)S_i^x + (qJ_yM_y + H_y)S_i^y + (qJ_zM_z + H_z)S_i^z], \tag{2}$$

in which $\beta = (kT)^{-1}$ is the inverse temperature, k is the Boltzmann constant set to one, q is the number of nearest neighbours (NN), and T is the absolute temperature. In addition, M_x, M_y and M_z are the magnetization components along x, y and z axes, respectively.

The spin-1/2 matrices are presented in terms of the Pauli spin matrices as $S^\mu = \frac{\hbar}{2}\sigma^\mu$ with μ set to x, y or z in three spin-dimensions and are given as

$$\sigma^x = \begin{pmatrix} 0 & 1 \\ 1 & 0 \end{pmatrix} \quad \sigma^y = \begin{pmatrix} 0 & -\mathrm{i} \\ \mathrm{i} & 0 \end{pmatrix} \quad \text{and} \quad \sigma^z = \begin{pmatrix} 1 & 0 \\ 0 & -1 \end{pmatrix}. \tag{3}$$

The constant $\frac{\hbar}{}$ is set to 1.0 for convenience, thus the spin-1/2 matrices become equal to Pauli spin matrices, i.e. $S^\mu = \sigma^\mu$. The Pauli spin matrices satisfy the following relations:

(i) the even powers of the Pauli spin matrices are equal to the unitary matrix

$$(\sigma^\mu)^{\mathrm{even}} = I = \begin{pmatrix} 1 & 0 \\ 0 & 1 \end{pmatrix}, \tag{4}$$

and their odd powers are equal to themselves, $(\sigma^\mu)^{\mathrm{odd}} = \sigma^\mu$;

(ii) they do not commute and satisfy the below relations

$$\sigma^x\sigma^y = -\sigma^y\sigma^x = \mathrm{i}\sigma^z = \mathrm{i}\begin{pmatrix} 1 & 0 \\ 0 & -1 \end{pmatrix},$$
$$\sigma^y\sigma^z = -\sigma^z\sigma^y = \mathrm{i}\sigma^x = \mathrm{i}\begin{pmatrix} 0 & 1 \\ 1 & 0 \end{pmatrix},$$
$$\sigma^z\sigma^x = -\sigma^x\sigma^z = \mathrm{i}\sigma^y = \mathrm{i}\begin{pmatrix} 0 & -\mathrm{i} \\ \mathrm{i} & 0 \end{pmatrix}, \tag{5}$$

which lead to

$$[\sigma^x, \sigma^y] = 2\mathrm{i}\sigma^z,\ [\sigma^y, \sigma^z] = 2\mathrm{i}\sigma^x \text{ and } [\sigma^z, \sigma^x] = 2\mathrm{i}\sigma^y; \tag{6}$$

(iii) they are anti-commutative:

$$\{\sigma^x, \sigma^y\} = 0,\ \{\sigma^y, \sigma^z\} = 0 \text{ and } \{\sigma^z, \sigma^x\} = 0. \tag{7}$$

It is well-known that the partition function is presented in terms of the exponential of Eq. (2), i.e. $-\beta\mathcal{H}_{\mathrm{MFA}}$,

$$Z_i = \mathrm{Tr}_{(i)}\left[\mathrm{e}^{-\beta\mathcal{H}_{\mathrm{MFA}}^{(i)}}\right]. \tag{8}$$

Therefore, for its calculation the exponential containing the spin matrices must be obtained. The exponential can be simplified as

$$\mathrm{e}^{-\beta\mathcal{H}_{\mathrm{MFA}}^{(i)}} = \mathrm{e}^{\beta[(qJ_xM_x + H_x)S_i^x + (qJ_yM_y + H_y)S_i^y + (qJ_zM_z + H_z)S_i^z]} = \mathrm{e}^{aS_i^x + bS_i^y + cS_i^z}, \tag{9}$$

with $a = \beta(qJ_xM_x + H_x)$, $b = \beta(qJ_yM_y + H_y)$ and $c = \beta(qJ_zM_z + H_z)$. The Taylor's series expansion of an exponential in the neighbourhood of $x = 0$ is given as

$$\mathrm{e}^x = \sum_{n=0}^{\infty} \frac{x^n}{n!} = 1 + x + \frac{x^2}{2!} + \frac{x^3}{3!} + \frac{x^4}{4!} + \dots, \qquad (10)$$

where x is some variable. But our exponential contains operators represented by Pauli spin matrices, thus one must be very careful in the expansion and follow the relations given in Eqs. (4–7). As a result, one obtains it as

$$\begin{aligned}\mathrm{e}^{aS_i^x + bS_i^y + cS_i^z} &= 1 + (aS_i^x + bS_i^y + cS_i^z) \\ &+ \frac{(aS_i^x + bS_i^y + cS_i^z)^2 (aS_i^x + bS_i^y + cS_i^z)}{2!} \\ &+ \frac{(aS_i^x + bS_i^y + cS_i^z)^2 (aS_i^x + bS_i^y + cS_i^z)}{3!} \\ &+ \frac{(aS_i^x + bS_i^y + cS_i^z)^2 (aS_i^x + bS_i^y + cS_i^z)^2}{4!} + \dots \qquad (11)\end{aligned}$$

After implementing the conditions (i) and (iii), and using $\alpha^2 = a^2 + b^2 + c^2$, the above exponential reaches a very nice form given as

$$\begin{aligned}\mathrm{e}^{aS_i^x + bS_i^y + cS_i^z} &= \left[1 + \frac{\alpha^2}{2!} + \frac{\alpha^4}{4!} + \frac{\alpha^6}{6!} + \dots\right] \mathrm{I} \\ &+ \frac{1}{\alpha}\left[1 + \frac{\alpha^3}{3!} + \frac{\alpha^3}{5!} + \frac{\alpha^7}{7!} + \dots\right](aS_i^x + bS_i^y + cS_i^z). \qquad (12)\end{aligned}$$

It can also be further simplified by recognizing the first term in the bracket as the cosh α and the last one as the sinh α:

$$\mathrm{e}^{aS_i^x + bS_i^y + cS_i^z} = \cosh\alpha\,\mathrm{I} + \frac{\sinh\alpha}{\alpha}(aS_i^x + bS_i^y + cS_i^z). \qquad (13)$$

The partition function is calculated as (details are given in the Appendix)

$$Z^{(i)} = \mathrm{Tr}[\mathrm{e}^{aS_i^x + bS_i^y + cS_i^z}] = 2\cosh\sqrt{a^2 + b^2 + c^2}. \qquad (14)$$

Now, with the knowledge of the partition function, the free energy can be calculated by the well-known formula

$$F = -kT\log(Z^{(i)}) = -kT\log\left(2\cosh\sqrt{a^2 + b^2 + c^2}\right). \qquad (15)$$

We are now ready to calculate the magnetization components. Let us start with the calculation of the zth component of magnetization M_z by using

$$M_z = \frac{\mathrm{Tr}[S_i^z \mathrm{e}^{-\beta\mathcal{H}_{\mathrm{MFA}}^{(i)}}]}{\mathrm{Tr}[\mathrm{e}^{-\beta\mathcal{H}_{\mathrm{MFA}}^{(i)}}]} = \frac{\mathrm{Tr}[S_i^z \mathrm{e}^{aS_i^x + bS_i^y + cS_i^z}]}{\mathrm{Tr}[\mathrm{e}^{aS_i^x + bS_i^y + cS_i^z}]}, \qquad (16)$$

in which the denominator is already calculated to be the partition function given in Eq. (14), and now the numerator must be obtained, the details of which are given in the Appendix, and found as

$$\begin{aligned}\mathrm{Tr} &= [S_i^z \mathrm{e}^{aS_i^x + bS_i^y + cS_i^z}] \\ &= \frac{2c}{\sqrt{a^2 + b^2 + c^2}} \sin\sqrt{a^2 + b^2 + c^2}. \qquad (17)\end{aligned}$$

Now inserting the results of Eqs. (14) and (17) into Eq. (16) gives the M_z as

$$M_z = \frac{c}{\sqrt{a^2 + b^2 + c^2}} \tanh\sqrt{a^2 + b^2 + c^2}. \qquad (18)$$

Similarly, the xth component of magnetization M_x is obtained by using

$$M_x = \frac{\mathrm{Tr}[S_i^x \mathrm{e}^{-\beta\mathcal{H}_{\mathrm{MFA}}^{(i)}}]}{\mathrm{Tr}[\mathrm{e}^{-\beta\mathcal{H}_{\mathrm{MFA}}^{(i)}}]} = \frac{\mathrm{Tr}[S_i^x \mathrm{e}^{aS_\mathrm{i}^x + bS_\mathrm{i}^y + cS_\mathrm{i}^z}]}{\mathrm{Tr}[\mathrm{e}^{aS_\mathrm{i}^x + bS_\mathrm{i}^y + cS_\mathrm{i}^z}]}, \qquad (19)$$

where the numerator of M_x is found from (see the Appendix)

$$\begin{aligned}&\mathrm{Tr}[S_i^x \mathrm{e}^{aS_\mathrm{i}^x + bS_\mathrm{i}^y + cS_\mathrm{i}^z}] = \\ &= \frac{2a}{\sqrt{a^2 + b^2 + c^2}} \sinh\sqrt{a^2 + b^2 + c^2}. \qquad (20)\end{aligned}$$

With the insertions of the results in Eqs. (14) and (20) into Eq. (19) the final form of M_x is found as

$$M_x = \frac{a}{\sqrt{a^2 + b^2 + c^2}} \tanh\sqrt{a^2 + b^2 + c^2}. \qquad (21)$$

Finally, the yth component of magnetization M_y is obtained by using

$$M_y = \frac{\mathrm{Tr}[S_i^y \mathrm{e}^{-\beta\mathcal{H}_{\mathrm{MFA}}^{(i)}}]}{\mathrm{Tr}[\mathrm{e}^{-\beta\mathcal{H}_{\mathrm{MFA}}^{(i)}}]} = \frac{\mathrm{Tr}[S_i^y \mathrm{e}^{aS_\mathrm{i}^x + bS_\mathrm{i}^y + cS_\mathrm{i}^z}]}{\mathrm{Tr}[\mathrm{e}^{aS_\mathrm{i}^x + bS_\mathrm{i}^y + cS_\mathrm{i}^z}]}, \qquad (22)$$

where the numerator of M_y is found from

$$\begin{aligned}&\mathrm{Tr}[S_i^y \mathrm{e}^{aS_\mathrm{i}^x + bS_\mathrm{i}^y + cS_\mathrm{i}^z}] = \\ &= \frac{2b}{\sqrt{a^2 + b^2 + c^2}} \sinh\sqrt{a^2 + b^2 + c^2}, \qquad (23)\end{aligned}$$

as can be seen in the Appendix.

After putting the results of Eqs. (14) and (23) into Eq. (22), the final magnetization component M_y is found as

$$M_y = \frac{b}{\sqrt{a^2+b^2+c^2}} \tanh\sqrt{a^2+b^2+c^2}. \quad (24)$$

It is clear that the coefficients $\frac{a}{\sqrt{a^2+b^2+c^2}}$, $\frac{b}{\sqrt{\ddot{u}^{\ddot{u}}+\ \ +}}$ and $\frac{c}{\sqrt{\ddot{u}^{\ddot{u}}+\ \ +}}$ for M_x, M_y and M_x in Eqs. (18), (21) and (24) play the role of weight functions since the sum of their squares is equal to one. Thus, their strengths determine which component of magnetization is dominant over the other one. The obtained formulations for M_x, M_y and M_z have a very nice form, but they are nonlinear and must be solved numerically, and here we have just employed simple iterations. Note also that the total magnetization is given as

$$M = \sqrt{M_x^2+M_y^2+M_z^2} = \tanh\sqrt{a^2+b^2+c^2}. \quad (25)$$

It is clear that the above equations are obtained for the FM case with $J_x > 0.0$, $J_y > 0.0$ and $J_z > 0.0$. For the AFM interactions with $J_x < 0.0$, $J_y < 0.0$ and $J_z < 0.0$, the lattice should be partitioned into sublattices A and B. In that case, the above equations must be modified as follows: the sublattice magnetizations now read as

$$M_x^A = M_x^A(M_x^B, M_x^B, M_x^B),$$
$$M_y^A = M_y^A(M_x^B, M_y^B, M_z^B),$$
$$M_z^A = M_x^A(M_x^B, M_y^B, M_z^B),$$
$$M_x^B = M_x^B(M_x^A, M_y^A, M_z^A),$$
$$M_y^B = M_y^B(M_x^A, M_y^A, M_z^A),$$
$$M_x^B = M_x^B(M_x^A, M_y^A, M_z^A), \quad (26)$$

the total magnetization now reads as

$$M = M^A + M^B$$
$$= \sqrt{(M_x^A)^2+(M_y^A)^2+(M_z^A)^2} +$$
$$+\sqrt{(M_x^B)^2+(M_y^B)^2+(M_z^B)^2} = \quad (27)$$
$$,= \left[\tanh\sqrt{a^2+b^2+c^2}\right]_A + \left[\tanh\sqrt{a^2+b^2+c^2}\right]_B.$$

and similarly the free energy becomes

$$F = F_A(M_x^A, M_y^A, M_z^A) + F_B(M_x^B, M_y^B, M_z^B), \quad (28)$$

thus the total magnetization and free energy for the AFM case is equal to the sum of the contributions coming from each sublattice A and B.

After having calculated all the equations for the FM and AFM cases, we are now ready to present their variations with respect to our parameter space, especially the temperature in the next section.

3. Illustrations

Now as the illustrations, we first study the thermal changes of magnetization components in detail to obtain the phase diagrams in possible planes for the XXX, XXZ and XYZ AFM models.

3.1. Thermal variations of magnetization components

As the first illustration of thermal variations of M_x, M_y and M_z for the AFM XXX case, we have presented in Fig. 1 that $J_x = J_y = J_z = J = -1.0$ for various values of $H_x = H_y = H_z = H$ with which the lines are labelled when $q = 4$. Since all the parameters are taken to be equal, the values of the weight functions are the same, thus all the components are equally probable leading to equal values of all. The critical temperatures at which the sublattice magnetizations become equal are the Neél temperatures, T_N, which persist to higher temperatures for lower H. The phase between the sublattice

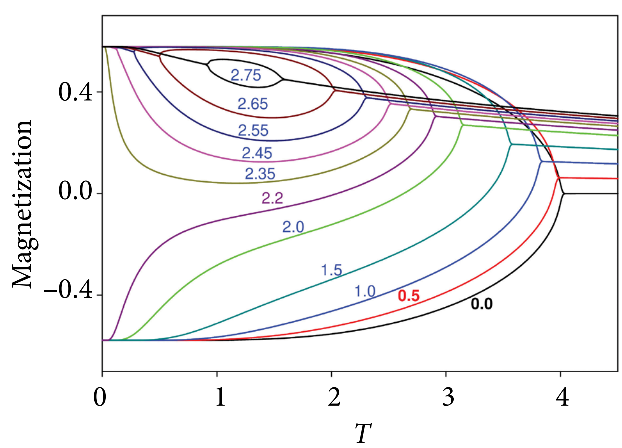

Fig. 1. Thermal variations of the magnetization components (M_x, M_y, M_z) for the sublattices A and B in the AFM XXX case when $J_x = J_y = J_z = J = -1.0$ for various values of $H_x = H_y = H_z = H$ and $q = 4$.

magnetizations is the AFM and afterwards it is the FM phase. Only for the $H = 0.0$ case, the FM and paramagnetic (PM) phases are separated at the T_N. When H is high enough, the sublattice magnetizations start with the FM phase for which $M_x = M_y = M_z$, then as T increases they are separated at the first T_N enclosing the AFM phase, and as T increases further they connect at the second T_N again and the components become equal corresponding to the FM phase. The double existence of T_N leads to the reentrant behaviour. When H values become high enough, all the magnetizations become equal only presenting the FM phase with no further existence of T_Ns. The next illustration, Fig. 2, is for the AFM XXZ model when $J_z = -0.5$, $H_x = H_y = H_z = H = 1.0$ and given values of $J_x = J_y = J = 0.0$, -0.25, -0.75 and -1.0. When $J_x = J_y$, it leads to $a = b$ and thus to equal values of $M_x = M_y$ shown with solid lines. Since $J_x \neq J_y = J_z = -0.5$, the M_z values, indicated with dotted-dashed lines, are also different but all have the same T_Ns. While $J_z > J$, then $M_z > M_x = M_y$ is true, and when $J_z < J$, $M_z < M_x = M_y$ holds as expected. It is also clear that as J increases towards $H = 1.0$, the T_Ns increase which is sensible. For the XYZ model, it is clear that as Js become larger the AFM regions and T_Ns increase.

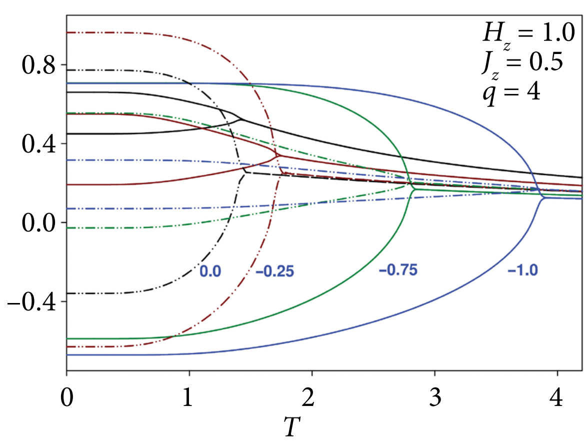

Fig. 2. Thermal variations of the magnetization components (M_x, M_y, M_z) for the sublattices A and B in the AFM XXZ model when $J_z = -0.5$, $H_x = H_y = H_z = H = 1.0$, $q = 4$ and the given values of $J_x = J_y = J = 0.0$, -0.25, -0.75 and -1.0.

3.2. *The phase diagrams*

The phase diagrams obtained only display Neél temperatures which separate the AFM and FM phases, and it is a second-order type phase transition. The spin-1/2 models do not display first-order phase transitions for the Ising models. The MF approach for the AFM models of this work similarly does not also display it. Again we illustrate the phase diagrams for the XXX, XXZ and XYZ models.

Figure 3 shows the phase diagrams obtained on the (H, T)-plane with $J_x = J_y = J_z = J = -1.0$ and $H_x = H_y = H_z = H$ for $q = 3$, 4 and 6 corresponding to honeycomb, square and simple cubic lattices. It shows that the T_Ns are higher for lower H and as H increases they decrease. The further decrease of H leads to bulgings in the T_N lines, i.e. the reentrant behaviour. The lower H parts of each line enclose the AFM phase while the right side is the FM phase. It is also clear that the T_N lines extend to higher T_Ns and Hs for higher q as expected from the spin models. Figure 1 of Ref. [5], Fig. 3 of Ref. [24], Fig. 1(a) of Ref. [18] and especially Figs. 3 and 4 of Ref. [4] display similar phase diagrams.

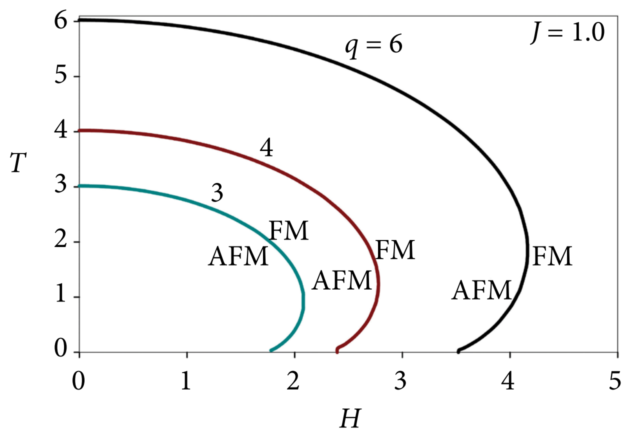

Fig. 3. Phase diagrams on the (H, T) planes for the given values of $q = 3$, 4 and 6 when $J_x = J_y = J_z = J = -1.0$ and $H_x = H_y = H_z = H$ for the XXX model.

The phase diagram for the XXZ model is presented on the (J, T) plane with $J_x = J_y = J$, $J_z = -0.5$, $q = 4$ and for given values of H as seen in Fig. 4. The T_N lines start from higher Ts at $J = 0.0$ for lower $H = 0.0$, 0.25, 0.5 and 1.0, and when $H > 1.0$ for shown values in the phase diagram, they start from $T = 0.0$ and higher Js for higher H. When $H \leq 1.0$, the T_N lines consist of AFM phase regions, otherwise they separate the FM phase (at lower J) from the AFM phase (at higher J). For the first three values of H when J_z is more negative than J, the T_N lines are almost straight under the rule of J_z. When H

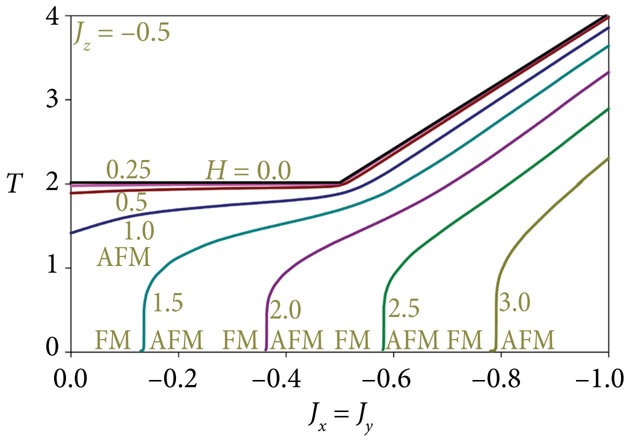

Fig. 4. Phase diagrams on the (J, T) planes for the XXZ model, i.e. $J_x = J_y = J$, when $J_z = -0.5$, $q = 4$ and the given values of $H_x = H_y = H_z = H$.

becomes compatible with J_z, i.e. $H = 1.0$, the T_N line goes downward. When $H > 1.0$, at low absolute J, first, the FM phase becomes dominant and as J absolutely increases the AFM phase appears. Then around $J = -0.5$, when compatible with $J_z = -0.5$, the T_N lines start increasing linearly and only the AFM phase remains. All these behaviours are very logical indicating the correctness of this work.

The final phase diagram displayed in Fig. 5 for the XYZ model on the (J_x, T) plane with $J_z = -0.5$, $H = 0.5$ and $J_y = 0.0, -0.25, -0.6, -0.7, -0.8, -0.9$ and -1.0 when $q = 4$ again. This figure is similar to the previous one, now the T_N lines always start from some nonzero values and they increase as J_y increases. The straight portion of the T_N lines persist to J_x about -0.5 when J_y is negatively smaller than J_x. For the values of J_y between -0.6 and -1.0

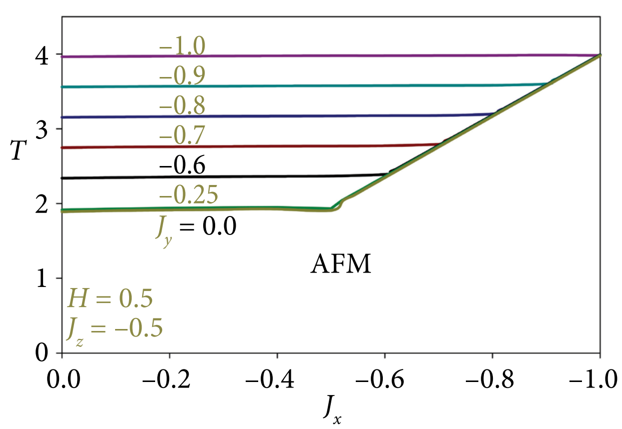

Fig. 5. Phase diagrams on the (J_x, T) planes for the XYZ model when $J_z = -0.5$, $H_x = H_y = H_z = H = 0.5$, $q = 4$ and the given values of J_y.

they persist until $J_x = J_y$. Afterwards they all linearly increase.

4. Conclusions

This work presents the formulations of the XYZ model for the spin-1/2 in terms of Pauli spin matrices and their exponentials. The main properties of Pauli spin matrices such as the commutation and anti-commutation rules are carefully applied to get very nicely formulated results for the partition function, free energy and magnetization components. Then their thermal changes are examined for various values of the coordination number for the XXX, XXZ and XYZ models for the AFM case. It is found that the model only displays the second-order phase transitions, i.e. Neél temperatures, with no indication of first-order phase transitions. It is found that the XXX model presents a reentrant behaviour. The work clearly indicates all the competition between the system parameters nicely. The regions of FM and AFM phase regions are observed which are separated by the T_N's. For comparisons with some other works, we were able to compare only the XXX model phase diagram with the works of Refs. [4, 5, 18, 24]. The similarities, especially the existence of a reentrant behaviour, agree with them. In the literature, it should be noted that we did not find any works approaching the MFA in a similar way except for the recent work [31].

Appendix

The details of the calculation for the partition function for Eq. (14):

$$Z^{(i)} = \mathrm{Tr}\left[e^{aS_i^x + bS_i^y + cS_i^z} \right] =$$

$$= \mathrm{Tr}\left[\cosh\alpha \; \mathrm{I} + \frac{\sinh\alpha}{\alpha}(aS_i^x + bS_i^y + cS_i^z) \right] =$$

$$= \mathrm{Tr}\left\{ \begin{array}{l} \cosh\alpha \begin{pmatrix} 1 & 0 \\ 0 & 1 \end{pmatrix} + \\ \dfrac{\sinh\alpha}{\alpha}\left[a\begin{pmatrix} 0 & 1 \\ 1 & 0 \end{pmatrix} + b\begin{pmatrix} 0 & -i \\ i & 0 \end{pmatrix} + c\begin{pmatrix} 1 & 0 \\ 0 & -1 \end{pmatrix} \right] \end{array} \right\} =$$

$$= \mathrm{Tr}\begin{pmatrix} \cosh\alpha + c\dfrac{\sinh\alpha}{\alpha} & (a - ib)\dfrac{\sinh\alpha}{\alpha} \\ (a + ib)\dfrac{\sinh\alpha}{\alpha} & \cosh\alpha - c\dfrac{\sinh\alpha}{\alpha} \end{pmatrix} =$$

$$= 2\cosh\alpha = 2\cosh\sqrt{a^2 + b^2 + c^2}. \tag{A.1}$$

The details of the calculation for M_z for Eq. (17):

$$\mathrm{Tr}\left[S_i^z \mathrm{e}^{aS_i^x+bS_i^y+cS_i^z}\right]$$

$$=\mathrm{Tr}\left\{S_i^z\left[\cosh\alpha\ \mathrm{I}+\frac{\sinh\alpha}{\alpha}(aS_i^x+bS_i^y+cS_i^z)\right]\right\}$$

$$=\mathrm{Tr}\left\{S_i^z\cosh\alpha+\frac{\sinh\alpha}{\alpha}[aS_i^zS_i^x+bS_i^zS_i^y+c(S_i^z)^2]\right\}$$

$$=\mathrm{Tr}\left\{S_i^z\cosh\alpha+\frac{\sinh\alpha}{\alpha}[a(\mathrm{i}S_i^y)+b(-\mathrm{i}S_i^x)+c\mathrm{I}]\right\}$$

$$=\mathrm{Tr}\begin{pmatrix}\cosh\alpha+c\frac{\sinh\alpha}{\alpha} & (a-\mathrm{i}b)\frac{\sinh\alpha}{\alpha}\\ -(a+\mathrm{i}b)\frac{\sinh\alpha}{\alpha} & -\cosh\alpha+c\frac{\sinh\alpha}{\alpha}\end{pmatrix}$$

$$=\frac{2c}{\alpha}\sinh\alpha=\frac{2c}{\sqrt{a^2+b^2+c^2}}\sinh\sqrt{a^2+b^2+c^2}. \quad \text{(A.2)}$$

The details of the calculation for M_x for Eq. (20):

$$\text{ü}\ \left[S_i^x\ {}^{aS_i^x+bS_i^y+cS_i^z}\right]$$

$$=\mathrm{Tr}\left\{S_i^x\left[\cosh\alpha\ \mathrm{I}+\frac{\sinh\alpha}{\alpha}(aS_i^x+bS_i^y+cS_i^z)\right]\right\}$$

$$=\mathrm{Tr}\left\{S_i^x\cosh\alpha+\frac{\sinh\alpha}{\alpha}[a(S_i^x)^2+bS_i^xS_i^y+cS_i^xS_i^z)]\right\}$$

$$=\mathrm{Tr}\left\{S_i^x\cosh\alpha+\frac{\sinh\alpha}{\alpha}[a\mathrm{I}+b(\mathrm{i}S_i^z)+c(-\mathrm{i}S_i^y)]\right\}$$

$$=\mathrm{Tr}\begin{pmatrix}(\alpha+\mathrm{i}b)\frac{\sinh\alpha}{\alpha} & \cosh a-c\frac{\sinh\alpha}{\alpha}\\ \cosh\alpha+c\frac{\sinh\alpha}{\alpha} & (a-\mathrm{i}b)\frac{\sinh\alpha}{\alpha}\end{pmatrix}$$

$$=\frac{2a}{\alpha}\sinh\alpha=\frac{2a}{\sqrt{a^2+b^2+c^2}}\sinh\sqrt{a^2+b^2+c^2}. \quad \text{(A.3)}$$

The details of the calculation for M_y for Eq. (23):

$$\mathrm{Tr}\left[S_i^y \mathrm{e}^{aS_i^z+bS_i^y+cS_i^z}\right]$$

$$=\mathrm{Tr}\left\{S_i^y\left[\cosh\alpha\ \mathrm{I}+\frac{\sinh\alpha}{\alpha}(aS_i^x+bS_i^y+cS_i^z)\right]\right\}$$

$$=\mathrm{Tr}\left\{S_i^y\cosh\alpha+\frac{\sinh\alpha}{\alpha}[aS_i^yS_i^x+b(S_i^y)^2+cS_i^yS_i^z]\right\}$$

$$=\mathrm{Tr}\left\{S_i^y\cosh\alpha+\frac{\sinh\alpha}{\alpha}[a(-\mathrm{i}S_i^z)+b\mathrm{I}+c(\mathrm{i}S_i^x)]\right\}$$

$$=\mathrm{Tr}\begin{pmatrix}(b+\mathrm{i}a)\frac{\sinh\alpha}{\alpha} & -\mathrm{i}\cosh\alpha+\mathrm{i}\ \frac{\sinh\alpha}{\alpha}\\ \mathrm{i}\cosh\alpha+\mathrm{i}c\frac{\sinh\alpha}{\alpha} & (b+\mathrm{i}a)\frac{\sinh\alpha}{\alpha}\end{pmatrix}$$

$$=\frac{2b}{\alpha}\sinh\alpha$$

$$=\frac{2b}{\sqrt{a^2+b^2+c^2}}\sinh(\sqrt{a^2+b^2+c^2}). \quad \text{(A.4)}$$

References

[1] R.I. Nepomechie and C. Wang, Boundary energy of the open XXX chain with a non-diagonal boundary term, J. Phys. A **47**, 032001 (2014), https://doi.org/10.1088/1751-8113/47/3/032001

[2] A. Degenhard, Nonperturbative real-space renormalization group scheme for the spin-1/2 XXX Heisenberg model, Phys. Rev. B **64**, 174408 (2001), https://doi.org/10.1103/PhysRevB.64.174408

[3] S. Jami and Z. Haqpanah, Magnetic field effects on quantum correlations for the XXX Heisenberg spin chain, J. Korean Phys. Soc. **72**, 743 (2018), https://doi.org/10.3938/jkps.72.743

[4] M.A. Neto, J.R. Viana, O.D.R. Salmon, E.B. Filho, and J.R. de Sousa, Phase transition induced by an external field in a three-dimensional isotropic Heisenberg antiferromagnet, Mod. Phys. Lett. B **32**, 1850390 (2018), https://doi.org/10.1142/S0217984918503906

[5] D.F. de Albuquerque, S.R.L. Alves, and A.S. de Arruda, Critical behavior in a random field classical Heisenberg model for amorphous systems, Phys. Lett. A **346**, 128 (2005), https://doi.org/10.1016/j.physleta.2005.07.060

[6] Y. Okabe and M. Kikuchi, Quantum Monte Carlo simulation of the spin-1/2 XXZ model on the square lattice, J. Phys. Soc. Japan **57**, 4351 (1988), https://doi.org/10.1143/JPSJ.57.4351

[7] M. Kikuchi and Y. Okabe, Exact diagonalization of the spin-1/2 XXZ model on the 4 × 4 square lattice, J. Phys. Soc. Japan **58**, 679 (1989), https://doi.org/10.1143/JPSJ.58.679

[8] D.J. Bukman, G. An and J.M.J. van Leeuwen, Cluster-variation approach to the spin-1/2 XXZ model, Phys. Rev. B **43**, 13352 (1991), https://doi.org/10.1103/PhysRevB.43.13352

[9] M. Kohno and M. Takahashi, Magnetization process of the spin-1/2 XXZ models on square and cubic lattices, Phys. Rev. B **56**, 3212 (1997), https://doi.org/10.1103/PhysRevB.56.3212

[10] J.R. de Sousa and J.A. Plascak, Phase transition in the three-dimensional anisotropic

Heisenberg antiferromagnetic model, Phys. Lett. A **237**, 66 (1997), https://doi.org/10.1016/S0375-9601(97)00795-0

[11] D.V. Dmitrieva, V.Ya. Krivnova, A.A. Ovchinnikova, and A. Langari, One-dimensional anisotropic Heisenberg model in the transverse magnetic field, Exp. Theor. Phys. **95**, 538 (2002), https://doi.org/10.1134/1.1513828

[12] J.R. de Sousa, N.S. Branco, B. Boechat, and C. Cordeiro, Quantum spin-1/2 two-dimensional XXZ model: an alternative quantum renormalization-group approach, Physica A **328**, 167 (2003), https://doi.org/10.1016/S0378-4371(03)00544-2

[13] T. Suzuki, Y. Tomita, and N. Kawashima, Magnetic properties of the spin-1/2 XXZ model on the Shastry-Sutherland lattice: Effect of long-range interactions, Phys. Rev. B **80**, 180405(R) (2009), https://doi.org/10.1103/PhysRevB.80.180405

[14] H. Moradmard, M.S. Naseri, and S. Mahdavifar, The 1D spin-1/2 XXZ model in transverse uniform and staggered magnetic fields, J. Supercond. Nov. Magn. **27**, 1265 (2014), https://doi.org/10.1007/s10948-013-2429-4

[15] S. Rufo, G. Mendonça, J.A. Plascak, and J.R. de Sousa, Order-disorder quantum phase transition in the quasi-one-dimensional spin-1/2 collinear antiferromagnetic Heisenberg model, Phys. Rev. E **88**, 034101 (2013), https://doi.org/10.1103/PhysRevE.88.034101

[16] Y.-Z. Huang, B. Xi, X. Chen, W. Li, Z.-C. Wang, and G. Su, Quantum phase transition, universality, and scaling behaviors in the spin-1/2 Heisenberg model with ferromagnetic and antiferromagnetic competing interactions on a honeycomb lattice, Phys. Rev. E **93**, 062110 (2016), https://doi.org/10.1103/PhysRevE.93.062110

[17] K. Morita and T. Tohyama, Magnetization plateau and supersolid phases in the spin-1/2 antiferromagnetic Heisenberg model on a tetragonally distorted fcc lattice, Phys. Rev. B **99**, 144417 (2019), https://doi.org/10.1103/PhysRevB.99.144417

[18] W.E.F. Parente, J.T.M. Pacobahyba, I.G. Araújo, M.A. Neto, J.R. de Sousa, and U. Akinci, Critical and reentrant behavior of the spin quantum 1/2 anisotropic Heisenberg antiferromagnet model with Dzyaloshinskii–Moriya interaction in a longitudinal magnetic field, J. Magn. Magn. Mater. **355**, 235 (2014), https://doi.org/10.1016/j.jmmm.2013.12.041

[19] W.E.F. Parente, J.T.M. Pacobahyba, M.A. Neto, I.G. Araújo, and J.A. Plascak, Spin-1/2 anisotropic Heisenberg antiferromagnet model with Dzyaloshinskii-Moriya interaction via mean-field approximation, J. Magn. Magn. Mater. **462**, 8 (2018), https://doi.org/10.1016/j.jmmm.2018.04.054

[20] J. Li and S. Lei, Thermodynamic properties of the spin-1/2 ferromagnetic Heisenberg chain with long-range interactions, Phys. Lett. A **372**, 4086 (2008), https://doi.org/10.1016/j.physleta.2008.03.005

[21] S. Sarkar, Quantum phase analysis of an anisotropic (XYZ) Heisenberg spin-1/2 chain under a uniform and staggered magnetic field, Int. J. Mod. Phys. B **23**, 3363 (2009), https://doi.org/10.1142/S0217979209052819

[22] J. Strečka, L. Čanová, and K. Minami, Spin-1/2 Ising-Heisenberg model with the pair XYZ Heisenberg interaction and quartic Ising interactions as the exactly soluble zero-field eight-vertex model, Phys. Rev. E **79**, 051103 (2009), https://doi.org/10.1103/PhysRevE.79.051103

[23] J. Cao, S. Cui, W.-L. Yang, K. Shi, and Y. Wang, Spin-1/2 XYZ model revisit: General solutions via off-diagonal Bethe ansatz, Nucl. Phys. B **886**, 185 (2014), https://doi.org/10.1016/j.nuclphysb.2014.06.026

[24] A.S. Filho, D.F. de Albuquerque, J.B.S. Filho, and T.S.A. Batista, Phase diagram of the classical Heisenberg model in a trimodal random field distribution, Physica A **461**, 133 (2016), https://doi.org/10.1016/j.physa.2016.05.047

[25] Y.H. Su, A.M. Chen, H. Wang, and C. Xiang, Quantum phase transition in the one-dimensional quantum Heisenberg XYZ model with Dzyaloshinskii–Moriya interaction, Eur. Phys. J. B **90**, 196 (2017), https://doi.org/10.1140/epjb/e2017-80077-8

[26] H.A. Zad, A. Zoshki, and M. Sabeti, Magnetic properties of an antiferromagnetic spin-1/2 XYZ

model in the presence of different magnetic fields: finite-size effects of inhomogeneity property, Commun. Theor. Phys. **71**, 1253 (2019), https://doi.org/10.1088/0253-6102/71/10/1253

[27] M.H. Ben Chakour, A. El Allati, and Y. Hassouni, Entangled quantum refrigerator based on two anisotropic spin-1/2 Heisenberg XYZ chain with Dzyaloshinskii–Moriya interaction, Eur. Phys. J. D **75**, 42 (2021), https://doi.org/10.1140/epjd/s10053-021-00056-0

[28] A. Hehn, N. van Well, and M. Troyer, High-temperature series expansion for spin-1/2 Heisenberg models, Comp. Phys. Commun. **212**, 180 (2017), https://doi.org/10.1016/j.cpc.2016.09.003

[29] E. Albayrak, Thermal entanglement in the anisotropic Heisenberg model with Dzyaloshinskii-Moriya interaction in an inhomogeneous magnetic field, Eur. Phys. J. B **72**, 491 (2009), https://doi.org/10.1140/epjb/e2009-00387-8

[30] E. Albayrak, Ferrmagnetic Heisenberg model with the Dzyaloshinskii-Moriya interaction, Cond. Matter Phys. **25**, 33701 (2022), https://doi.org/10.5488/CMP.25.33701

[31] E. Albayrak, The XYZ model by the series expansion of exponentials for spin matrices in the mean-field approximation, Eur. Phys. J. Plus **138**, 228 (2023), https://doi.org/10.1140/epjp/s13360-023-03802-y

XYZ MODELIS VIDUTINIO LAUKO ARTINYJE, NAUDOJANT PAULIO SUKINIO MATRICAS

E. Albayrak

Erdžijo universiteto Fizikos fakultetas, Kaiseris, Turkija